Diffusion-limited aggregation with power-law pinning

H. G. E. Hentschel,[1,*] M. N. Popescu,[2,3,†] and F. Family[1,‡]

[1]*Department of Physics, Emory University, Atlanta, Georgia 30322, USA*
[2]*Max-Planck-Institut für Metallforschung, Heisenbergstrasse 3, D-70569 Stuttgart, Germany*
[3]*Institut für Theoretische und Angewandte Physik, Universität Stuttgart, Pfaffenwaldring 57, D-70569 Stuttgart, Germany*

Using stochastic conformal mapping techniques we study the patterns emerging from Laplacian growth with a power-law decaying threshold for growth $R_N^{-\gamma}$ (where R_N is the radius of the N-particle cluster). For $\gamma > 1$ the growth pattern is in the same universality class as diffusion limited aggregation (DLA), while for $\gamma < 1$ the resulting patterns have a lower fractal dimension $D(\gamma)$ than a DLA cluster due to the enhancement of growth at the hot tips of the developing pattern. Our results indicate that a pinning transition occurs at $\gamma = 1/2$, significantly smaller than might be expected from the lower bound $\alpha_{min} \approx 0.67$ of multifractal spectrum of DLA. This limiting case shows that the most singular tips in the pruned cluster now correspond to those expected for a purely one-dimensional line. Using multifractal analysis, analytic expressions are established for $D(\gamma)$ both close to the breakdown of DLA universality class, i.e., $\gamma \lesssim 1$, and close to the pinning transition, i.e., $\gamma \gtrsim 1/2$.

I. INTRODUCTION

Nonequilibrium growth models leading naturally to self-organized fractal structures, such as diffusion limited aggregation (DLA) [1], are of continuing interest due to their relevance for many important physical processes including dielectric breakdown [2], electrochemical deposition [3,4], and Laplacian flow [5].

A powerful method, namely, iterated stochastic conformal mapping [6,7], has been already successfully applied to generate and analyze DLA [8,9] and Laplacian [10] growth patterns in two dimensions. This has provided an alternative way to address many of the important open questions related to pattern formation in DLA in two dimensions, one of these being the existence of minimal fields for growth at the boundary of the growing cluster. In previous work [11] we studied the properties induced by a *fixed*, material dependent critical field E_c for growth, and showed that in the presence of such a threshold all clusters ultimately become pinned and, in addition, this simple constraint has remarkable consequences for the resulting patterns—the rich, branched structure of DLA is replaced by a much lower-dimensional shape consisting of a few surviving branches.

In this paper we address a similar, but significantly more important question because of its relationship to the multifractal spectrum of DLA, that of what happens when there exists a critical field for growth on the boundary of the cluster, field decaying like $R_N^{-\gamma}$ as the cluster increases in size. We shall call this model the "γ model." As we will show below, as γ decreases from $\gamma > 1$ toward a critical value $\gamma = 1/2$ (which corresponds to the most singular possible behavior for the Laplacian field, i.e., that occurring at the tip of a line), there is a continuous transition from DLA toward

lower-dimensional shapes for which the multifractal spectrum is necessarily different from that of DLA. We study this transition in terms of the fractal dimension $D(\gamma)$ of the emerging patterns, and we derive analytic expressions for the behavior of $D(\gamma)$ in the range $\gamma \lesssim 1$ where the DLA universality class breaks down and $\gamma \gtrsim 1/2$ close to the pinning transition.

II. MODEL AND THEORETICAL BACKGROUND

Witten and Sander [1] have shown that the growth probability at any point s on the boundary of a DLA cluster of length L is given by the harmonic measure $P(s) = |\nabla V(s)| / \int_0^L ds' |\nabla V(s')|$, where $V(\mathbf{r})$ obeys Laplace's equation $\nabla^2 V = 0$ subject to the boundary conditions $V = 0$ on the (evolving) boundary of the cluster and $V \sim \ln r$ as $r \to \infty$ (corresponding to a uniform flux of particles far away from the cluster).

The model we study is a variant of the two-dimensional DLA growth model described above in which growth is disallowed at points on the cluster boundary where the probability for growth is smaller than a critical value $R_N^{-\gamma}$, where R_N (the exact meaning will be defined later) is the radius of the N particle cluster, i.e.,

$$P_{grow}(s) = \begin{cases} \dfrac{|\nabla V(s)|}{\displaystyle\int_0^L \theta[\gamma - \alpha(s')] |\nabla V(s')| ds'}, & |\nabla V| > R_N^{-\gamma} \\ 0, & |\nabla V| < R_N^{-\gamma}, \end{cases}$$

(1)

where $\alpha(s')$ is the multifractal exponent at point s' on the cluster boundary, L is the length of the boundary, and the step function $\theta(\gamma - \alpha(s'))$ ensures that only those regions of the cluster boundary obeying $|\nabla V(s')| > R_N^{-\gamma}$ contribute to the normalization integral. Estimates of this integral will be very important in our analysis of the fractal dimension of the

—————
*Electronic address: phshgeh@physics.emory.edu
†Electronic address: popescu@mf.mpg.de
‡Electronic address: phyff@emory.edu

growing "γ cluster." Since we need to calculate the harmonic measure on a freely evolving interface, this is handled by using conformal mapping techniques [6,8]. The method was presented in great detail in Refs. [6,8], and thus here we will just briefly review the main results.

The basic idea is to follow the evolution of the conformal mapping $z = \Phi^{(n)}(\omega)$ of the exterior of the unit circle in a mathematical ω plane onto the complement of the cluster of n particles in the physical z plane rather than directly the evolution of the cluster's boundary. The initial condition is chosen to be $\Phi^{(0)}(\omega) = \omega$. The process of adding a new "particle" of constant shape and linear scale $\sqrt{\lambda_0}$ to the cluster of $(n-1)$ particles at a position s which is chosen randomly according to the harmonic measure is described via a function $\phi_{\lambda,\theta}(\omega)$, where

$$
\begin{aligned}
\phi_{\lambda,0}(\omega) = \omega^{1-a} \Bigg\{ & \frac{(1+\lambda)}{2\omega}(1+\omega)\Bigg[1+\omega \\
& + \omega \left(1 + \frac{1}{\omega^2} - \frac{2}{\omega}\frac{1-\lambda}{1+\lambda} \right)^{1/2} \Bigg] - 1 \Bigg\}^{a} \phi_{\lambda,\theta}(\omega) \\
= & e^{i\theta}\phi_{\lambda,0}(e^{-i\theta}\omega),
\end{aligned} \tag{2}
$$

which conformally maps the unit circle to the unit circle with a bump of linear size $\sqrt{\lambda}$ localized at the angular position θ [6]. The shape of the bump depends on the parameter a. Following the analysis in Ref. [8], we have used $a = 0.66$ througout this paper, as we believe the large scale asymptotic properties will not be affected by the microscopic shape of the added bump.

The conformal map for an n-particle cluster $\Phi^{(n)}(\omega)$ can be built by adding one particle to an $(n-1)$-particle cluster $\Phi^{(n-1)}(\omega)$, resulting in the recursive dynamics,

$$
\Phi^{(n)}(\omega) = \Phi^{(n-1)}(\phi_{\lambda_n,\theta_n}(\omega)), \tag{3}
$$

which can be solved in terms of iterations of the elementary bump map $\phi_{\lambda_n,\theta_n}(\omega)$,

$$
\Phi^{(n)}(\omega) = \phi_{\lambda_1,\theta_1} \circ \phi_{\lambda_2,\theta_2} \circ \cdots \circ \phi_{\lambda_n,\theta_n}(\omega). \tag{4}
$$

In Eqs. (3) and (4) the angle $\theta_n \in (0, 2\pi]$ at step n is randomly chosen since the harmonic measure on the real cluster translates to a uniform measure on the unit circle in the mathematical plane,

$$
P(s)ds = \frac{d\theta}{2\pi}, \tag{5}
$$

and

$$
\lambda_n = \frac{\lambda_0}{|\Phi^{(n-1)\prime}(e^{i\theta_n})|^2}, \tag{6}
$$

is chosen in order to ensure that the size of the bump in the physical z plane is $\sqrt{\lambda_0}$. Since $\sqrt{\lambda_0}$ is a natural length scale in the problem, it can be scaled out by measuring all the lengths in terms of it. We reemphasize here that although the

composition, Eq. (4), appears at first sight to be a standard iteration of stochastic maps, this is not so because the order of iterations is inverted—the last point of the trajectory is the inner argument in this iteration. As a result the transition from $\Phi^{(n-1)}(\omega)$ to $\Phi^{(n)}(\omega)$ is achieved by composing the n former maps, Eq. (4), starting from a different seed. Finally, identifying [8] the radius R_n of the growing pattern with the coefficient $F_1^{(n)} = \Pi_{i=1}^{n}(1+\lambda_i)^a$ in the Laurent expansion of $\Phi^{(n)}$,

$$
\Phi^{(n)}(\omega) = F_1^{(n)}\omega + F_0^{(n)} + F_{-1}^{(n)}\omega^{-1} + F_{-2}^{(n)}\omega^{-2} + \cdots, \tag{7}
$$

the constraint to grow only at values of θ which obey Eq. (1) translates into

$$
\frac{1}{|[\Phi^{(n-1)}]'(e^{i\theta})|} > (F_1^{(n-1)})^{-\gamma}. \tag{8}
$$

This constraint is implemented as follows. At step n, θ_n is choosen from a uniform distribution in $(0, 2\pi]$, independent of previous history. If it obeys the constraint given by Eq. (8) accept this value of θ_n, otherwise repeat until the constraint is obeyed.

III. RESULTS AND DISCUSSION

For the model defined in Sec. II one would expect the resultant patterns to have fractal shapes which depend on γ, and in order to characterize these shapes we will focus on the scaling behavior of the first Laurent coefficient $F_1^{(n)}$. Following the arguments in Ref. [8], for a given value γ one expects a scaling law of the form

$$
F_1^{(n)} \sim n^{1/D(\gamma)}, \tag{9}
$$

where $D(\gamma)$ is the effective fractal dimension of the resulting cluster.

We have simulated the model defined in Sec. II for a number of values γ in the range $1/2 \le \gamma \le 1.6$ and we have calculated $F_1^{(n)}$ as an average over 100 clusters (for $\gamma > 0.65$), and, respectively, over 20 clusters (for $\gamma \le 0.65$) of size $N = 40\,000$. In Fig. 1 we show typical clusters of size $N = 40\,000$ for $\gamma = 1.20$, 0.75, and 0.55, respectively. It can be easily seen that the rich, branched structure of the cluster at $\gamma = 1.20$ changes, as γ decreases toward $\gamma = 0.55$, into a much lower-dimensional shape with only a few branches surviving. This can be intuitively understood by considering the effect the pinning probability $R_n^{-\gamma}$ has on the multifractal spectrum of the cluster. From multifractal scaling [12–14] we know that the interface of a fully developed DLA cluster consists of sets of $\mathcal{N}_{DLA}(\alpha) \sim R_n^{f_{DLA}(\alpha)}$ sites with growing probabilities $|\nabla V| \sim R_n^{-\alpha}$, and we will assume that such a structure is also valid for the clusters grown with pinning probability $R_n^{-\gamma}$. As growth proceeds, the lowest probability sites (large α), normally deep in the fjords, will be pinned first, with the hot tips surviving longest, leading to "pruning" of the branches where the tips have a singularity $\alpha > \gamma$.
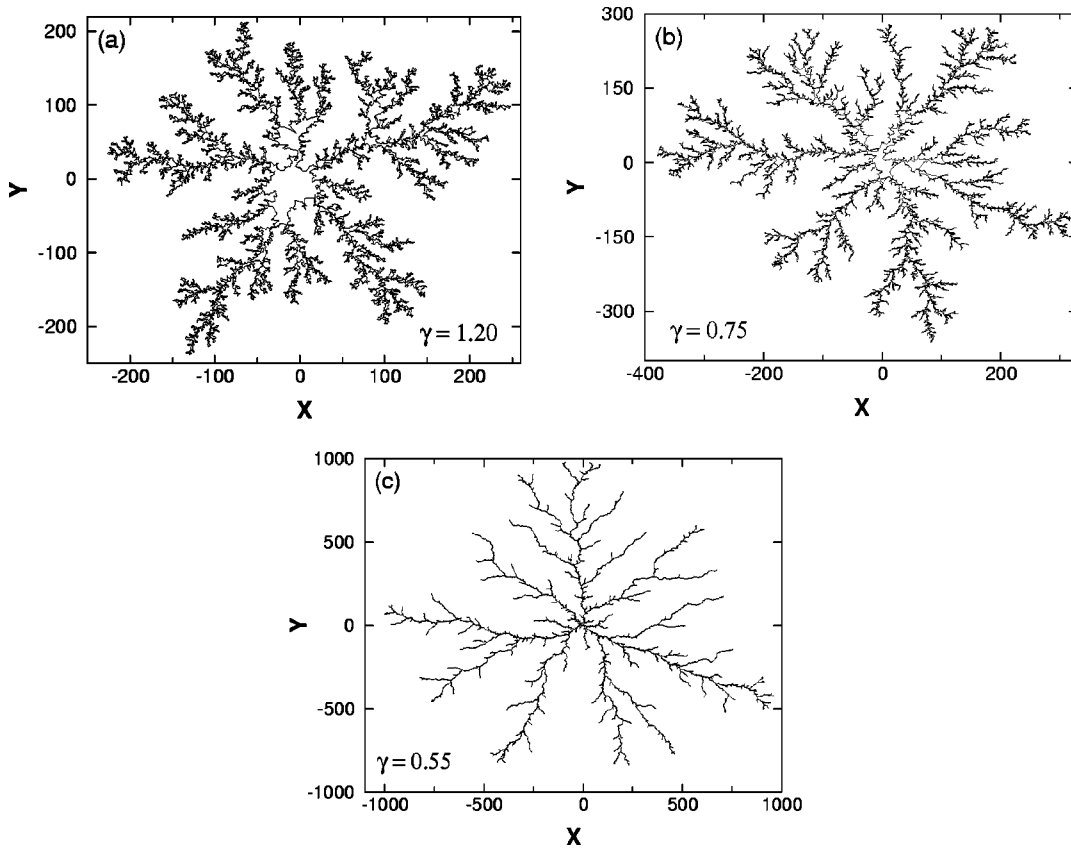
FIG. 1. Typical clusters (size $N = 40\,000$) grown with (a) $\gamma = 1.20$, (b) $\gamma = 0.75$, and (c) $\gamma = 0.55$, respectively.

As anticipated, for all the values $0.5 \leq \gamma \leq 1.2$ that we have tested the coefficient $F_1^{(n)}$ has a clear power-law dependence on the size n, as shown in Fig. 2(a). Assuming the exponent $1/D(\gamma)$ to be related to a fractal dimension as given by Eq. (9), the dependency $D(\gamma)$ [shown in Fig. 2(b)] is obtained from a power-law fit to the data. It can be seen that at values of $\gamma \gtrsim 1$ the behavior is close to that of a DLA

cluster, i.e., $D(\gamma > 1) \rightarrow D_{DLA} \simeq 1.71$, while for $\gamma \gtrsim 1/2$ the behavior of the radius $F_1^{(n)}$ tends to n, i.e., $D(\gamma \rightarrow 1/2) \rightarrow 1$, thus the behavior of a growing line.

In order to understand these results theoretically let us begin with a very simple argument based on the assumption that the clusters have a multifractal spectrum in the sense described above, in that the interface consists of sets of
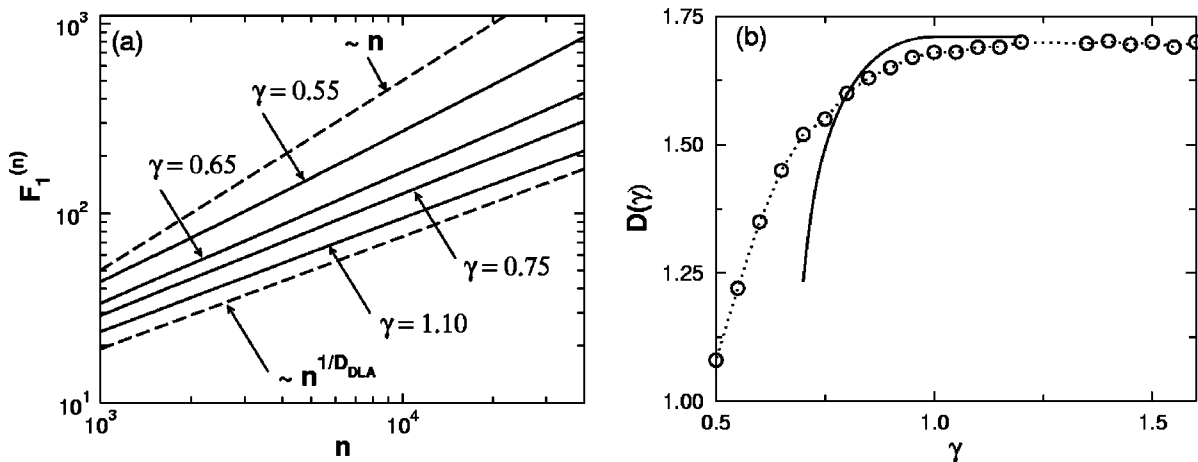

FIG. 2. (a) $F_1^{(n)}$ as a function of n for clusters grown with $\gamma = 1.20$, 0.75, 0.65, and 0.55, respectively (log-log plot). Also shown (dashed lines) are the limit cases of a DLA cluster, $F_1^{(n)} \sim n^{1/D_{DLA}}$, where $D_{DLA} = 1.71$, and of a line cluster $F_1^{(n)} \sim n$, respectively. (b) The effective fractal dimension $D(\gamma)$ obtained from $F_1^{(n)} \sim n^{1/D(\gamma)}$ as a function of γ (circles). The dotted line is just a guide to the eye. The solid line is the theoretical prediction [Eq. (13)] with $f_{DLA}(\gamma)$ from Ref. [15].
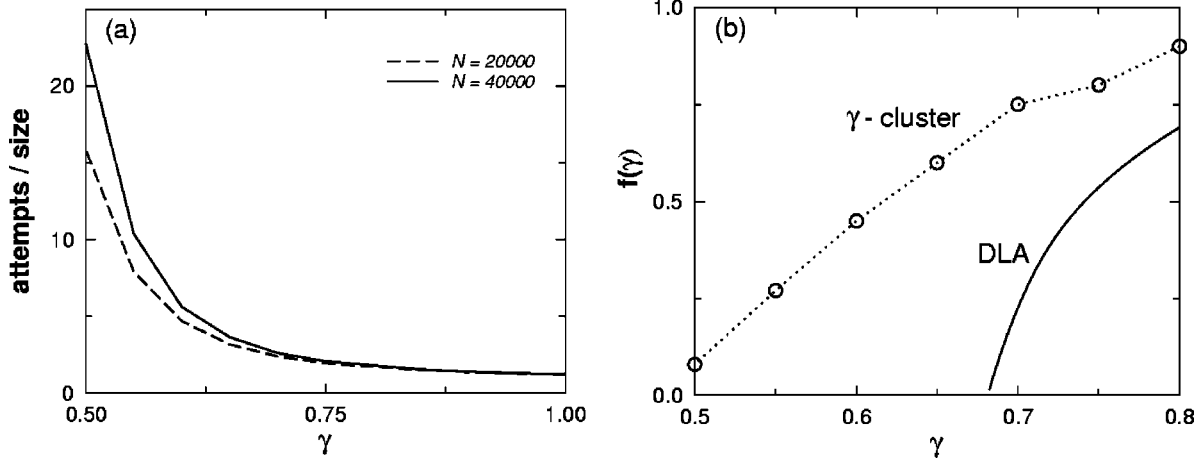
FIG. 3. (a) Average number of attempts for growing clusters of sizes $N = 20\,000$ (dashed line) and $N = 40\,000$ (solid line), scaled by the actual size of the cluster, respectively, as function of γ (b) The multifractal spectrum $\tilde{f}(\gamma)$ from Eq. (15) (symbols) in comparison with the multifractal spectrum of DLA (solid line) from Ref. [15].

$\mathcal{N}_\gamma(\alpha) \sim R_n^{f_\gamma(\alpha)}$ sites with growth probabilities $|\nabla V| \sim R_n^{-\alpha}$. Since the constraint will cutoff growth at regions in the cluster with exponents in the range $\alpha > \gamma$ of the multifractal spectrum, we can write down the following equation for the rate of growth of the cluster in the presence of the barrier in terms of the rate of growth of a DLA (no barrier for growth) cluster

$$\left(\frac{dR}{dN}\right)_\gamma \sim \left(\frac{dR}{dN}\right)_{DLA} \left(\int_{\alpha_{min}}^{\gamma} d\alpha\, C(\alpha) R^{f_\gamma(\alpha)-\alpha}\right)^{-1},$$

where $f(\alpha_{min}) = 0$. The enhancement of growth comes from Eq. (1) together with the estimate

$$\int_0^L \theta(\gamma - \alpha(s)) |\nabla V(s')| ds' \sim \int_{\alpha_{min}}^{\gamma} d\alpha\, C(\alpha) R^{f_\gamma(\alpha)-\alpha}. \tag{10}$$

Now, we know that the harmonic measure is concentrated at $\alpha = 1$, and thus for $\gamma > 1$ the integral is dominated by the value of the integrand at $\alpha = 1$, while for $\gamma \lesssim 1$ it is dominated by the value at γ, and thus

$$\left(\frac{dR}{dN}\right)_\gamma \sim \left(\frac{dR}{dN}\right)_{DLA} \times \begin{cases} K(\gamma) & \text{for } \gamma > 1 \\ R^{\gamma - f_\gamma(\gamma)} & \text{for } \gamma \lesssim 1, \end{cases} \tag{11}$$

where $K(\gamma)$ is some constant independent of N. Equation (11) therefore implies

$$D(\gamma) = \begin{cases} D_{DLA} & \text{for } \gamma > 1 \\ D_{DLA} + f_\gamma(\gamma) - \gamma & \text{for } \gamma \lesssim 1. \end{cases} \tag{12}$$

For the case where $\gamma \lesssim 1$, i.e., close to the breakdown in the DLA universality class, we may assume that the multifractal spectrum of the cluster is only weakly perturbed from its value in DLA and therefore $f_\gamma(\gamma) \approx f_{DLA}(\gamma)$, or

$$D(\gamma) = \begin{cases} D_{DLA} & \text{for } \gamma > 1 \\ D_{DLA} + f_{DLA}(\gamma) - \gamma & \text{for } \gamma \lesssim 1. \end{cases} \tag{13}$$

This prediction may be tested using the recently computed $f_{DLA}(\alpha)$ spectrum [15]. The results are shown in Fig. 2(b) (solid line), and it can be seen that for $\gamma \simeq 1$ the theoretical predictions are indeed close to the measured values $D(\gamma)$. The discrepancies at smaller values of γ can be attributed to the fact that the multifractal spectrum of the cluster is not exactly the one of DLA, and when $\gamma \to 1/2$, as we will now discuss, it actually may be expected to deviate significantly from that of a DLA.

For $\gamma \gtrsim 1/2$, the change in the multifractal spectrum from that for DLA is significant. For example, it is known [15,16] that for the DLA spectrum $\alpha_{min} \simeq 0.67$, while we see that growth continues significantly below this value, with $\alpha_{min} = 1/2$ being the asymptotic limit. Our simulations show strong evidence for this limit, as can be seen in Fig. 3(a): the average number of attempts for growing clusters of sizes $N = 20\,000$ and $N = 40\,000$ (scaled by the actual size of the cluster) exhibits a steep increase as $\gamma \to 0.5$.

We shall assume that for these highly pruned γ-clusters there is a well defined limiting form for the multifractal spectrum $f_\gamma(\alpha)$ defined for $1/2 < \alpha < \gamma$ and obeying $f_\gamma(1/2) = 0$, which is a monotonically increasing function of γ. Defining $\tilde{f}(\gamma) = f_\gamma(\gamma)$, we can use a reasoning similar to that used by Turkevich and Sher [16] in their estimate of the fractal dimension of DLA to estimate $\tilde{f}(\gamma)$. The idea is that for $\gamma \gtrsim 1/2$ only the "hottest" tips contribute to growth, and thus one can write

$$\left(\frac{dR}{dN}\right)_\gamma \sim P_{max} \sim R^{-1/2} \left(\int_{1/2}^{\gamma} d\alpha\, C(\alpha) R^{f_\gamma(\alpha)-\alpha}\right)^{-1}$$

$$\sim R^{-1/2 - \tilde{f}(\gamma) + \gamma}, \tag{14}$$

where the last relation follows from the fact that the integral is dominated by the value of the integrand at γ. Thus, we obtain

$$\tilde{f}(\gamma) = D(\gamma) + \gamma - 3/2. \tag{15}$$

Since from simulations we know the values $D(\gamma)$, Eq. (15) (which is valid for $\gamma \gtrsim 0.5$) allows the calculation of the upper multifractal exponent $\tilde{f}(\gamma)$. As shown in Fig. 3(b), the pinning threshold $R^{-\gamma}$ leads to a shifting of the multifractal spectrum for $\alpha < \gamma$ to the left, i.e., $f_\gamma(\alpha) > f_{DLA}(\alpha)$ (more hot tips, and larger fields at those hot tips, due to pruning).

These results can be intuitively understood as a flow of singularities away from γ (which acts as an unstable fixed point of the dynamics). For any particular value $\alpha_0 < \gamma$, what happens while the cluster evolves is that screening is reduced compared to DLA and therefore there is a flow of singularities $\alpha_0 \to \alpha_1$ with $\alpha_1 < \alpha_0$. In addition, new singularities with $\alpha < \alpha_{\min}^{(DLA)}$, can be created. Thus, we would expect that the number of singularities $\mathcal{N}_\gamma(\alpha_1) \approx \mathcal{N}_{DLA}(\alpha_0)$ or

$$f_\gamma(\alpha_1(\alpha_0)) \approx f_{DLA}(\alpha_0). \tag{16}$$

On the other hand for $\alpha_0 > \gamma$ the singularity flow $\alpha_0 \to \alpha_1$ can only act toward an increase $\alpha_1 \geq \alpha_0$ since such points can never grow and thus can only either keep their original singularity or get a higher value of α during growth.

IV. CONCLUSIONS

Using the stochastic conformal mapping techniques we have studied the patterns emerging from Laplacian growth with a power-law decaying threshold for growth $R_N^{-\gamma}$, $\gamma \geq 1/2$. We have shown that due to the enhancement of growth at the hot tips as γ decreases the growth evolves from patterns in the DLA universality class for $\gamma > 1$ to clusters with a lower fractal dimension $D(\gamma)$ for $\gamma < 1$ due to the enhancement of growth at the hot tips. We have presented evidence that $\gamma = 1/2$, corresponding to the singularities at the tip of a purely one-dimensional (line) growth pattern, is the lower limit for growth, with all clusters becoming ultimately pinned for $\gamma < 1/2$. By using multifractal analysis, we have proposed analytic expressions for $D(\gamma)$ for both $\gamma \lesssim 1$ near the breakdown of the DLA universality class and near the pinning transition $\gamma \gtrsim 1/2$. Finally, we have shown that in the small γ range the multifractal spectrum of the resulting cluster is significantly changed from that of a DLA. We have suggested that this change may be due to a flow of singularities with γ acting as an unstable fixed point of the dynamics, but further work will be necessary to fully elucidate this point.

[1] T.A. Witten, Jr. and L.M. Sander, Phys. Rev. Lett. **47**, 1400 (1981).

[2] L. Niemeyer, L. Pietronero, and H.J. Wiesmann, Phys. Rev. Lett. **52**, 1033 (1984).

[3] R.M. Brady and R.C. Ball, Nature (London) **309**, 225 (1984).

[4] M. Matsushita, M. Sano, Y. Hayakawa, H. Honjo, and Y. Sawada, Phys. Rev. Lett. **53**, 286 (1984).

[5] L. Paterson, Phys. Rev. Lett. **52**, 1621 (1984).

[6] M.B. Hastings and L.S. Levitov, Physica D **116**, 244 (1998).

[7] M.B. Hastings, Phys. Rev. E **55**, 135 (1997).

[8] B. Davidovich, H.G.E. Hentschel, Z. Olami, I. Procaccia, L.M. Sander, and E. Somfai, Phys. Rev. E **59**, 1368 (1999).

[9] B. Davidovich and I. Procaccia, Phys. Rev. Lett. **85**, 3608 (2000).

[10] F. Barra, B. Davidovitch, A. Levermann, and I. Procaccia, Phys. Rev. Lett. **87**, 134501 (2001).

[11] H.G. E Hentschel, M.N. Popescu, and F. Family, Phys. Rev. E **65**, 036141 (2002).

[12] H.G.E. Hentschel and I. Procaccia, Physica D **8**, 435 (1983).

[13] T.C. Halsey, P. Meakin, and I. Procaccia, Phys. Rev. Lett. **56**, 854 (1986).

[14] T.C. Halsey, M.H. Jensen, L.P. Kadanoff, I. Procaccia, and B. Shraiman, Phys. Rev. A **33**, 1141 (1986).

[15] M.H. Jensen, A. Levermann, J. Mathiesen, and I. Procaccia, Phys. Rev. E **65**, 046109 (2002).

[16] L. Turkevich and H. Sher, Phys. Rev. Lett. **55**, 1026 (1985).